Lung Perfusion Imaging with Monosized Biodegradable Microspheres

Urs O. Häfeli,*,† Katayoun Saatchi,† Philipp Elischer,† Ripen Misri,† Mehrdad Bokharaei,† N. Renée Labiris,‡ and Boris Stoeber§

Faculty of Pharmaceutical Sciences and Departments of Mechanical Engineering and Electrical and Computer Engineering, The University of British Columbia, Vancouver, British Columbia, Canada, and Department of Medicine, Divisions of Respirology and Clinical Pharmacology, McMaster University, Hamilton, Ontario, Canada

Received September 20, 2009; Revised Manuscript Received January 27, 2010

After intravenous injection, particles larger than red blood cells will be trapped in the first capillary bed that they encounter. This is the principle of lung perfusion imaging in nuclear medicine, where macroaggregated albumin (MAA) is radiolabeled with ^{99m}Tc, infused into a patient's arm vein, and then imaged with gamma scintigraphy. Our aim was to evaluate if monosized microspheres could replace ^{99m}Tc-MAA. Biodegradable poly(L-lactide) microspheres containing chelating bis(picolylamine) end groups were prepared by a flow focusing method on a microfluidic glass chip and were of highly homogeneous size (9.0 ± 0.4 μm). The microspheres were radiolabeled with $[^{99m}Tc(H_2O)_3(CO)_3]^+$ and then evaluated in mice for lung perfusion imaging. Fifteen minutes after injection, 79.6 ± 3.8% of the injected activity was trapped in the lungs of mice. Monosized biodegradable radioactive microspheres are, thus, appropriate lung perfusion imaging agents. Other sizes of these highly uniform microspheres have the potential to improve diagnostic and therapeutic approaches in diverse areas of medicine.

Introduction

Micrometer-sized particles, microspheres, are essential tools for diagnostic imaging in nuclear medicine and for the therapeutic radiation treatment of tumors in radiation oncology.[1,2] Smaller nanometer-sized particles, nanoparticles, find use as magnetic resonance imaging (MRI) contrast agents in radiology.[3,4] The full diagnostic and therapeutic potential of both particle types is, however, constrained by technical obstacles that prevent them from being reliably directed to a target site after intravascular administration. If these limitations can be overcome, micro- and nanoparticles could become highly effective intravascular tools in applications such as organ-specific gene therapy, site-directed hemolysis in stroke patients, and the controlled release of highly active anticancer drugs in cancer patients over days to months after targeted intravascular delivery to a tumor.[5,6]

Effective passive targeting strongly depends on particle size and uniformity.[7] Particle diameter determines which organ or tissue traps the injected particles (e.g., lymph, bone marrow, liver, or lungs), while particle uniformity determines the extent of trapping. Thus, we postulate that use of particles of a specific and uniform size will lead to complete uptake and retention in an organ or tissue of interest upon intravascular injection. Control over the size distribution of particles is also important as large particles may unintentionally clog small blood vessels, leading to embolism. Because larger particles can also result from the agglomeration of smaller ones, minimizing agglomeration is, thus, another key to successful targeting. Agglomeration can be minimized by providing a hydrophilic particle surface, for example, by pegylation.[8]

Current production methods for microspheres cannot provide the necessary narrow size distribution of biocompatible particles, yielding instead particles with a wide size distribution with typical coefficients of variation (C.V.) above 40%. This is especially true for nontoxic, biodegradable microspheres made from the polyesters poly(lactide-*co*-glycolide) (PLGA) and poly(lactide) (PLA). It was our aim to narrow the size distribution for microspheres made from these materials by employing a combination method of flow focusing and solvent extraction to prepare monosized PLA microspheres. Hydrodynamic flow focusing was first described in 1975,[9] but it took more than 20 years before the fabrication methods developed in microsystem technology and the advances in microfluidics allowed for the successful production of monosized liquid droplets and gas bubbles with this method.[10] Using this method, small uniform droplets that incorporate therapeutic drugs and the polymeric matrix material can be formed. The lipophilic solvent is then removed (extracted) from the uniform droplets and diffuses into the surrounding aqueous phase, leaving drug-laden uniform polymer microspheres.[11,12]

Herein, we report the successful preparation of monosized, nontoxic, biodegradable microspheres formulated to minimize agglomeration with the flow focusing method. The particles' in vivo potential for size-specific organ uptake is illustrated with 9.0 μm particles that are shown to accumulate in the lungs after intravenous injection. The particles are, thus, successful lung perfusion agents and are compared to conventionally used ^{99m}Tc-radiolabeled macroaggregated albumin (MAA).[13]

Materials and Methods

Preparation of Microspheres. A combination of microfluidic flow focusing[12,14,15] and solvent extraction[16,17] was used to prepare mono-

* To whom correspondence should be addressed. Tel.: (604) 822-7133. Fax: (604) 822-3035. E-mail: uhafeli@interchange.ubc.ca.
† Faculty of Pharmaceutical Sciences, The University of British Columbia.
‡ McMaster University.
§ Departments of Mechanical Engineering and Electrical and Computer Engineering, The University of British Columbia.

10.1021/bm9010722
Published on Web 02/09/2010

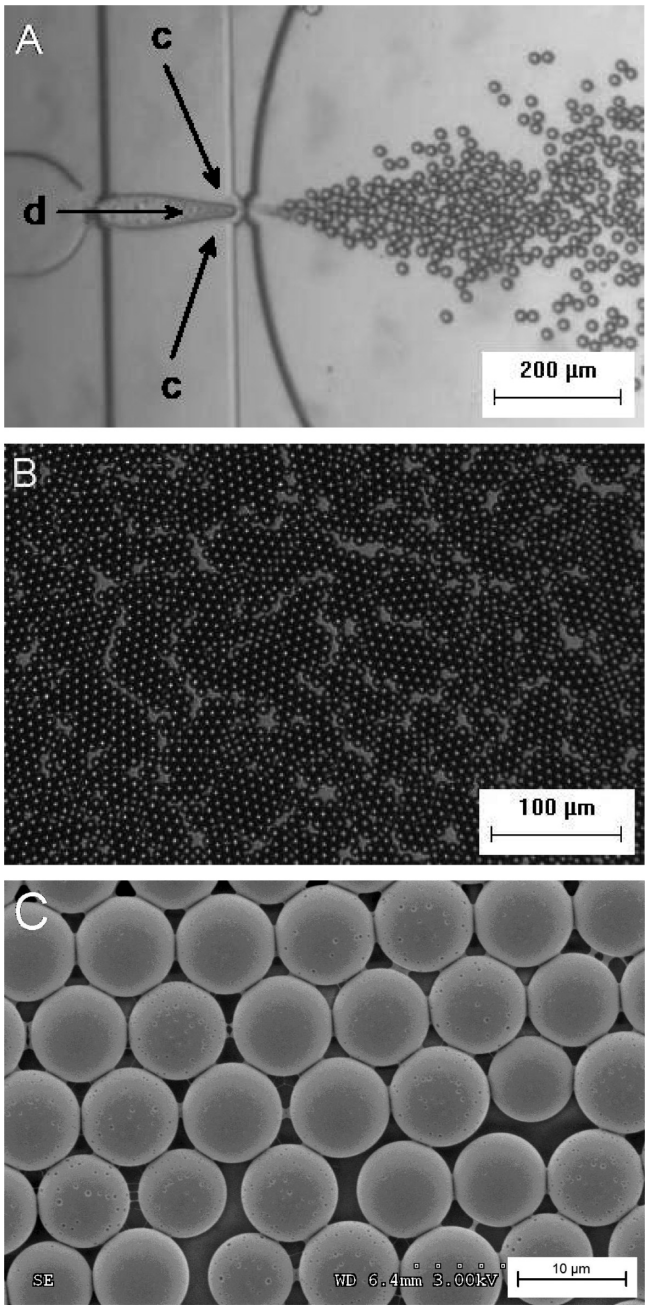

Figure 1. (A) Microscopic picture of the glass microfluidic chip during the production of microspheres [**c**: continuous phase with a 2% (w/v) aqueous PVA solution; **d**: disperse phase with a 10% (w/v) PLA solution in chloroform]. (B) Microspheres formed after complete solvent extraction. (C) Scanning electron microscopy (SEM) picture of the same microspheres.

sized microspheres from the FDA-approved biodegradable polymer PLA. A chloroform solution **d** (Figure 1A) containing the dissolved polymer blend of commercial PLA, custom-made bis(picolylamine)-functionalized PLA for $[^{99m}Tc(CO)_3]^+$ coordination,[18] and pegylated polycaprolactone[19] $MePEG_{17}$-*b*-PCL_{10} to obtain a more hydrophilic particle surface was pumped through a central microfluidics glass channel and then through an orifice. Simultaneously, the continuous phase **c** (Figure 1A), consisting of an aqueous PVA solution, was pumped through the same orifice but at a 15× higher volumetric flow rate. The flow rate differential of the two phases focuses the disperse phase into a thin thread which breaks into droplets of identical size upon leaving the orifice. Chloroform then diffuses out of the droplets into the surrounding water phase because it is very slightly soluble in water (saturation concentration of 0.8% (w/v) chloroform in water). Monosized microspheres (Figure 1B,C) form once the polymer concentration in the droplet exceeds its solubility product, a process that is further helped by pumping the freshly formed microspheres into a large volume of stirred water solution where the rest of the chloroform is extracted.

A microfluidic system was prepared on a glass chip that provided the appropriate geometry for the flow focusing method. This geometry permitted to reach the necessary flow conditions that guarantee the formation of uniform droplets that subsequently form uniform microspheres. The microchannels were isotropically etched 20 μm deep into a borofloat glass substrate (Micralyne, Edmonton, AB, Canada). The critical narrow microchannel constriction was achieved through the isotropic etching process by merging of two neighboring etch pits. The width of the resulting orifice was about 40 μm (Figure 1A). The glass lid, which was unstructured except for drilled access holes, was then fusion-bonded to the etched substrate to form closed flow channels.

Disperse and continuous phases were pumped by a separate syringe pump each (BS-8000; Braintree Scientific, Braintree, MA). The pumps were connected to the microchannel glass slide with Teflon tubing (Upchurch Scientific, Oak Harbour, WA). A third, reverse-pumping syringe pump then transported the newly produced microspheres into a water-filled vial where constant solvent extraction and evaporation was maintained by a magnetic stirrer.

The continuous phase that stabilizes the jet and droplet formation during the flow focusing process consisted of a 2% (w/v) polyvinyl alcohol (PVA; MW 13−23 kDa, 87−89% hydrolyzed, Sigma Aldrich, Oakville, Ontario, Canada) solution and was pumped at a flow rate of 10 μL/min, while the disperse phase was a 5% (w/v) PLA/ligand−polymer/PCL-PEG solution and was pumped through the central channel (Figure 1A) at a flow rate of 0.67 μL/min. The polymer mixture consisted of 92% L-PLA (Resomer L104, Boehringer Ingelheim), 3% $MePEG_{17}$-*b*-PCL_{10},[19] and 5% bis(picolylamine)-functionalized PLA prepared in our lab according to a published procedure.[18] To guarantee formation of microspheres of a uniform size, constant flow conditions of both phases were necessary. Microsphere collection therefore began only after the phases had been pumping for 20 min and the flow was judged by optical observation to be stable. Droplet formation was observed using an inverted stage microscope (AE31, Motic, Richmond, BC, Canada; Figure 1A). After 1 h of stirring, microspheres were centrifuged three times and washed with distilled water. For imaging, samples were then gold sputtered and images were obtained using a Hitachi S-3000N scanning electron microscope at an accelerating voltage of 3.0 kV. Before application, the microspheres were lyophilized to remove residual traces of solvents and for storage.

Cell Toxicity of Ligand Microspheres. The in vitro cytotoxicity of the chelating microspheres was tested using a modified cell viability assay.[20] The MTT (3-[4,5-dimethylthiazol-2yl]-2,5-diphenyltetrazolium bromide) assay is a colorimetric assay for which 3000 tumor cells were plated, in 100 μL of media, into each well of a 96-well plate and incubated for 48 h. The epidermoid carcinoma cell line A431 was chosen as a sensitive marker for toxicity and has in our own lab been used to detect potentially toxic effects much quicker than nonmalignant epithelial cell lines would.[21] A total of 100 μL of a suspension containing 0.03, 0.1, 0.3, and 1.0 mg/mL of pure L-PLA microspheres or the chelating microspheres in DMEM media were added and incubated for another 48 h. A total of 20 μL of a 5 mg/mL MTT solution was added and incubated for three more hours. Viable cells take up the yellow MTT dye into their mitochondria and metabolize it there into blue formazan crystals. As a control, 150 μL of PBS at pH 7.4 was added to cells in eight of the wells. The supernatant in each well was aspirated and 150 μL of dimethyl sulfoxide (DMSO) was added to solubilize the cells and MTT crystals. After 30 min on a rocker shaker, all crystals had dissolved and the blue color was read in a multiwell scanning spectrophotometer at 570 nm. The cell viability was calculated by comparing the sample absorption to the one of the control cells, which was by definition 100%. Polymeric microspheres were considered toxic if the difference between cell growth inhibition

of control and exposed cells was statistically significant at the 5% level, as determined by a *t*-test.

Radiolabeling of Microspheres. Radiolabeling of the microspheres was achieved by first preparing 740 MBq of $[^{99m}Tc(H_2O)_3(CO)_3]^+$ (^{99m}Tc-tricarbonyl) with an Isolink kit (generously provided by Mallinckrodt) and then adding 74 MBq of this precursor to a suspension of 2 mg of monosized microspheres in 100 μL of water. The mixture was heated to 75 °C for 30 min in a Thermomixer R (Eppendorf, Mississauga, Ontario, Canada) shaking at 1000 rpm. The labeling efficiency was determined by centrifugation of the microspheres and dividing the total activity minus the activity of the supernatant over the total activity. Stability studies including a cysteine challenge are described in detail in a previous study.[22]

Microsphere Biodistribution. Biodistribution experiments were carried out in compliance with the ethics committee at the University of British Columbia in a group of six male C57Bl6 mice (UBC Life Sciences) that weighed 26.7 ± 1.7 g. The mice received an intravenous tail vein injection of 150 μL of the microsphere suspensions containing 0.2 mg of microspheres radiolabeled with 5.5 MBq of ^{99m}Tc each. After 15 min, the animals were sacrificed and the organs were removed, weighed, and their activity determined using a Packard Cobra II auto gamma-counter. Results were expressed as the percentage of the injected dose per organ and per gram of tissue (%ID/g), and the tumor-to-blood ratios calculated from the %ID/g values.

MicroSPECT/CT Imaging. The biodistribution of the radiolabeled microspheres was investigated by microSPECT/CT imaging on an X-SPECT instrument (Gamma Medica, Northridge, CA; now Siemens) at McMaster's Centre for Preclinical and Translational Imaging (MCPTI) in Hamilton, Ontario, Canada. The animal care committee at McMaster University approved this pilot study. Microspheres were labeled as explained above just before the imaging studies at the Nuclear Medicine Department's Radiopharmacy. In an additional step before injection, the ^{99m}Tc-microspheres were spun down in a centrifuge at 2500 g for 5 min, the supernatant was discarded and saline was added. As this was a proof of concept lung perfusion study, only one test and one control female BALB/C mouse were used. The test mouse received 7.4 MBq of the radiolabeled microspheres in 100 μL of saline by intravenous tail vein injection. After 5 min, a SPECT scan (32 projections for 40 s each using a 1 mm pinhole collimator) was performed under isoflurane anesthesia in supine position, followed by a CT scan (512 projections). The control mouse was anaesthetized using isoflurane and administered 17.9 MBq of ^{99m}Tc-labeled macroaggregated albumin (MAA, Bristol Myers Squibb) in 200 μL of saline by tail vein injection. After 5 min, a SPECT scan (same parameters as above) was acquired, followed by a CT scan (1024 projections).

The SPECT/CT images were graphed and analyzed with the medical image data examiner software AMIDE V0.9.0 (available online free of charge at http://amide.sourceforge.net).

Results

Using a combination of flow focusing and solvent extraction on a microfluidics glass chip, we prepared monodisperse microspheres (Figure 1) with a diameter of 9.00 ± 0.44 μm. The size distribution was very narrow, with a coefficient of variation of 4.9% (Figure 2). This variation is equivalent to a polydispersity index (PDI) of 1.006.

While L-PLA is FDA approved, it was not known yet if the PLA-ligand derivative could also be considered nontoxic. To determine biocompatibility, a cell viability assay of the final microspheres was performed and compared to the pure L-PLA microspheres (Figure 3). A small dose-dependent decrease of viability was visible at the largest tested particle concentration of 1 mg/mL, but this was the case for both microsphere preparations, with no statistical difference between them (*t*- test, $p = 12.3\%$). Clinical perfusion tests would be done with less than 10 mg of the radiolabeled microspheres, a concentration

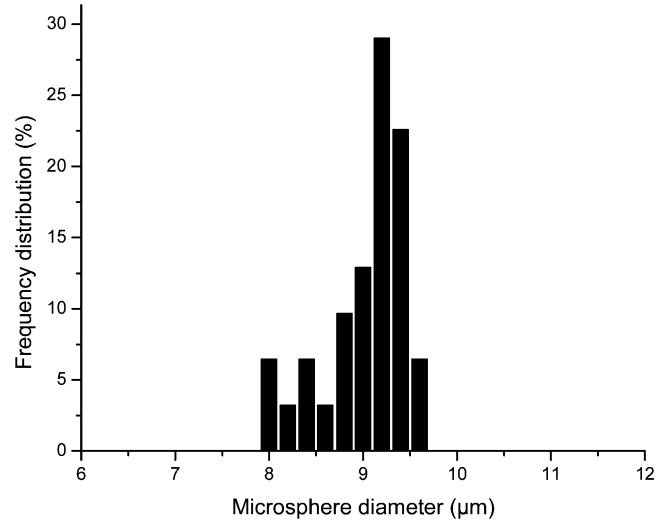

Figure 2. Size distribution of the biodegradable PLA microspheres measured from several scanning electron microscopy pictures such as Figure 1C ($n = 186$).

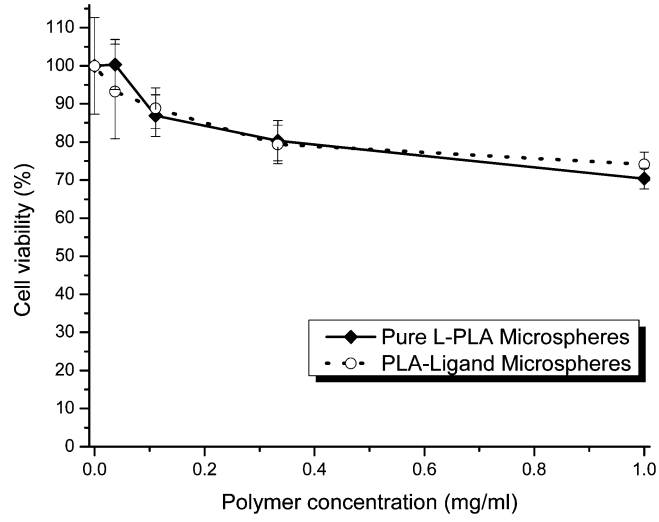

Figure 3. Effect of pure PLA microspheres and PLA-ligand microspheres on cell viability of A431 epidermoid carcinoma cells using an MTT cell viability assay.

that would be less than the 0.11 mg/mL concentration also tested in this MTT assay (Figure 3). At that concentration, no statistical difference was found between control cells and cells with added PLA or chelating microspheres, respectively (*t*-test, $p = 13.2$ vs 8.4%, respectively).

Based on the particle size and narrow size distribution, it is expected that, following intravenous tail vein injection into a mouse, such particles will bypass the liver, pass through the right heart chambers, and enter the lungs, where they encounter the pulmonary capillary bed. At that point, because their size exceeds that of the typical mouse lung capillary (i.e., 5.7 μm),[23] they would be retained by the first capillaries they encounter. Indeed, we show that this was the case in this proof of concept study.

The exact polymer composition used to make the microspheres is based on a previous study where we could show that 5% of the ligand polymer in addition to 92% of the nonchelating "bulk" polymer L-PLA is a large enough amount to enable high radiolabeling efficiencies.[18,22] The missing 3% of the polymer weight consist of a pegylated polymer, which prevents agglomeration of the particles and allows for optimal distribution.[22]

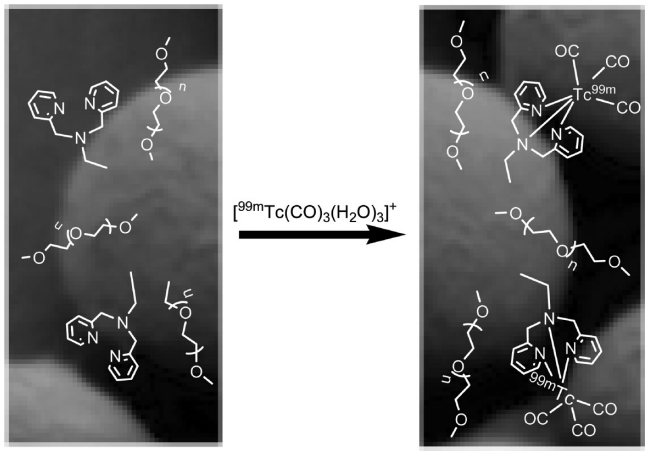

Figure 4. Schematic of the microsphere surface with ligand and poly(ethylene glycol) groups before and after radiolabeling with the ^{99m}Tc(I)-tricarbonyl approach.

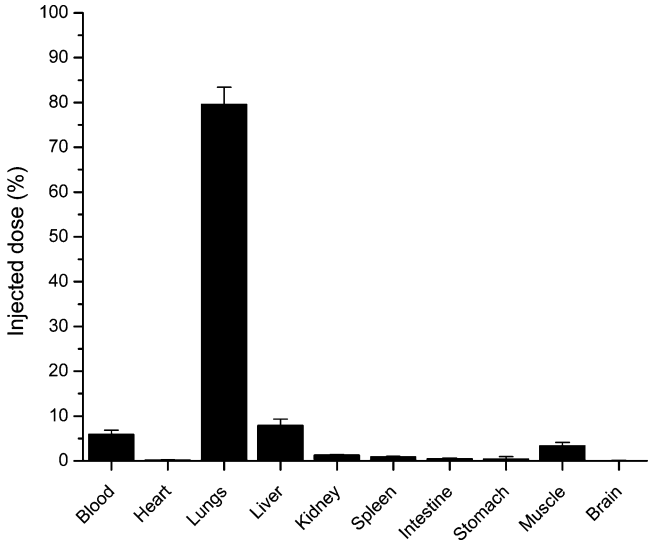

Figure 5. Biodistribution of ^{99m}Tc-microspheres in C57Bl/6 mice measured 15 min after tail vein injection ($n = 6$).

A schematic of the microsphere structure and its radiolabeling step is shown in Figure 4. The microspheres were radiolabeled with $[^{99m}Tc(CO)_3]^+$ with a radiolabeling efficiency of 94.7%. The microspheres were injected into the tail veins of a group of normal mice. After 15 min, the mice were sacrificed and the radioactivity biodistribution measured (Figure 5 and Table 1).

In addition to the conventional biodistribution study, we also visualized and compared the ^{99m}Tc-microspheres and ^{99m}Tc-MAA in a single animal each using microSPECT/CT imaging. The radiolabeling efficiency for the ^{99m}Tc-microspheres used in this imaging experiment was 95.5%. In both cases, most particles were retained and distributed in a homogeneous manner throughout the lungs (Figures 6A and 8A).

The area of interest (AOI) analysis of the ^{99m}Tc-microsphere images showed that almost all activity (99.4%) was found in the lung region, with only very small activities found in thyroid (0.1%) and liver (0.5%; Figure 6B). This excellent lung uptake of the radiolabeled microspheres after lung perfusion without any instability, that is, no radioactivity observable in any other organ or tissue, is likely due to the additionally done centrifugation of microspheres shortly before injection, which must have removed any unbound activity. Another way of visualizing this concentrated lung uptake is to surface render the imaging data (Figure 7).

The control mouse that received the ^{99m}Tc in the form of radiolabeled MAA also showed high (96.0%) and homogeneous lung uptake (Figure 8A). Quantitatively, however, slightly more of the radioactivity was detected in liver (3.4%) and thyroid (0.6%; Figure 8B). No statistical difference can be inferred from these single animal results, they only served to visualize the results obtained in the biodistribution study.

Discussion

Our experiments demonstrated that monosized microspheres become trapped in the capillary bed of the lungs after intravenous tail vein injection into a mouse very similar to the trapping of macroaggregated albumin. This makes these microspheres candidates for diagnostic lung perfusion studies where it could replace MAA, a human blood product that carries the risk of virus and prion transmission. Our monosized biodegradable microspheres, on the other hand, are made using the biodegradable FDA-approved polymer PLA as the matrix material. PLA, and the very similar polymer poly(lactide-*co*-glycolide (PLGA) that can be used interchangeably, have an excellent record of biocompatibility, biodegradability, and nonimmunogenicity.[24−28] From our here performed initial cell viability studies, the addition of 8 wt % of two biodegradable polymer derivatives to the PLA matrix material does not seem to change the particles' overall toxic properties.

In terms of biodegradability, both MAA and PLA are comparable: Once lodged in the capillaries, MAA and PLA will both slowly break down into smaller protein and polyester fragments and finally be absorbed and recycled by the body in the form of amino acids and lactic acid, respectively. The kinetics of these degradation processes is, however, expected to be different. MAA has been described as having a biological half-life of 55 days,[29] while L-PLA used here degrades within 3−6 months at 37 °C.[30] No specific biodegradation studies with the microspheres used here have been performed yet and should be done in the future. However, we stored a suspension of the microspheres at 4 °C for 9 months, and light microscopic comparison to similarly long stored pure L-PLA microspheres showed no difference in their surface structure and overall size. If shorter degradation times are desired, then a faster degrading PLGA polymer could be used as the matrix material. Currently, the fastest degrading clinical grade PLGA 50:50 polymers (PLGA Medisorb) with an inherent viscosity of around 0.1 dL/g break down into their soluble components within 1−2 weeks.

In addition to the materials for the preparation of particles being less risky and more available, the most important advantage of the monosized microspheres over MAA is their extremely narrow size distribution. The particle size was chosen so that capillaries, but not arterioles, were embolized. Human precapillary vessels (arterioles) have a diameter of 13 μm.[31] The used microspheres with an average size of 9 μm will thus exclusively clog capillaries, and a regional pulmonary embolism can be avoided. The total injected amount of 0.2 mg of microspheres, or 250000 particles, is expected to be nontoxic, as typical lungs contain 280 billion capillaries,[32] and less than 0.0001% of their capacity is thus embolized. Important for the prevention of embolism is also the incorporation of 3% of a pegylated polymer into the matrix material of the microspheres. As shown in a separate investigation with smaller microspheres of between 0.5 to 2 μm in diameter,[22] this pegylated polymer was able to completely prevent aggregation of the microspheres in the blood in vivo. Microspheres made from purely PLA, however, agglomerated and accumulated to a significant extent

Table 1. Activity Distribution of the ^{99m}Tc-Microspheres 15 Min after Tail Vein Injection into C57Bl/6 Mice ($n = 6$)

	injected dose (%) ± SD		organ/blood ratio ± SD		injected dose (%/g) ± SD	
blood	5.90	0.95	1.00	0.00	2.50	0.09
heart	0.18	0.05	0.35	0.09	0.98	0.30
lungs	79.61	3.79	103.47	27.10	333.65	83.79
liver	7.88	1.44	1.72	0.04	4.29	0.14
kidney	1.28	0.11	0.94	0.02	2.34	0.03
spleen	0.87	0.14	3.08	0.39	7.69	0.82
intestine	0.48	0.15	0.20	0.04	0.50	0.10
stomach	0.39	0.51	0.99	1.24	2.48	3.11
muscle	3.34	0.77	0.07	0.01	0.18	0.04
brain	0.07	0.03	0.04	0.01	0.10	0.03

in the lungs of the animals.[22] Other authors have also reported the need for making polyester microspheres more hydrophilic on their surface to prevent agglomeration.[33] Their best lung uptake was reported after making PLGA microspheres with an addition of 8% of the surface-active poloxamer 188 (see also Table 2).

Monosized microspheres made by flow focusing are perfect spheres, while MAA forms irregularly shaped aggregates. No changes take place in the size and shape of the microspheres during the radiolabeling step. We have shown this in a previous investigation using scanning electron microscopy with smaller, but not monosized, particles made from the same materials.[22] For MAA, the radiolabeling can lead to nonoptimal particle size distributions. To exclude the feared large aggregates, ^{99m}Tc-MAA is normally checked with a hemocytometer under a light microscope before use. The package insert of MAA typically describes the particles' size distribution as 90% being sized between 10 and 90 μm, with no particles larger than 150 μm. Most manufacturers' MAA are within these limits, although a comparison study by Mallol and Diaz found in some cases particles as small as 7.2 μm.[34]

For optimal imaging, it is not only necessary that the carrier, here the microspheres or MAA, have the optimal properties for uptake in the target organ, but also that the radioactive label, here ^{99m}Tc, stays tightly bound to the carrier for the time between radiolabeling and injection plus the length of the procedure. The biodistribution study (Table 1 and Figure 5) showed the major uptake of the particles in the lungs. There was, however, a larger than expected amount of activity based on the radiolabeling efficiency found in the liver and in the blood. Some of it might be due to unbound $[^{99m}Tc(H_2O)_3(CO)_3]^+$, which is rapidly excreted through the kidneys and, thus, is visible in the initial minutes in the blood pool, the kidney, and also the liver.[22] However, because only 5.3% of the activity was not microsphere bound after radiolabeling, as determined by centrifugation and separation of the supernatant, the rest of the activity must come from somewhere else. We have previously confirmed the good stability of the ^{99m}Tc-tricarbonyl chelation by the polymer microspheres in cysteine challenge and in vivo studies.[18,22] The small and highly stable $[^{99m}Tc(CO)_3]^+$ core seems to stay polymer-bound in Tc(I) form.[35] For this reason, we think that some of the liver uptake might be due to pulmonary anastomoses, connections between the arterial and the venous side in addition to the capillary bed, in the C57Bl/6 mice used for the biodistribution study. Anastomoses will allow larger particles to bypass the capillary bed and travel to the liver, where they are captured. Interestingly, this was not seen at all in the balb/C mice that we used in the imaging experiment (Figures 6 and 7). It might also be that the capillaries of the two types of mice have a slightly different diameter and that our chosen size of microspheres should be increased by a few micrometers to maximize capillary trapping.

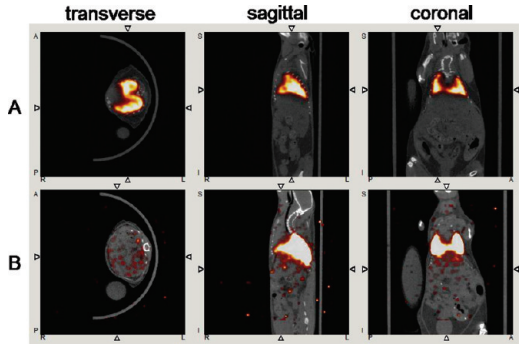

Figure 6. (A) Lung perfusion SPECT scan using biodegradable ^{99m}Tc-microspheres. (B) The same data but shown in the transverse direction through the liver with a much more sensitive radioactivity threshold to depict thyroid and liver activity.

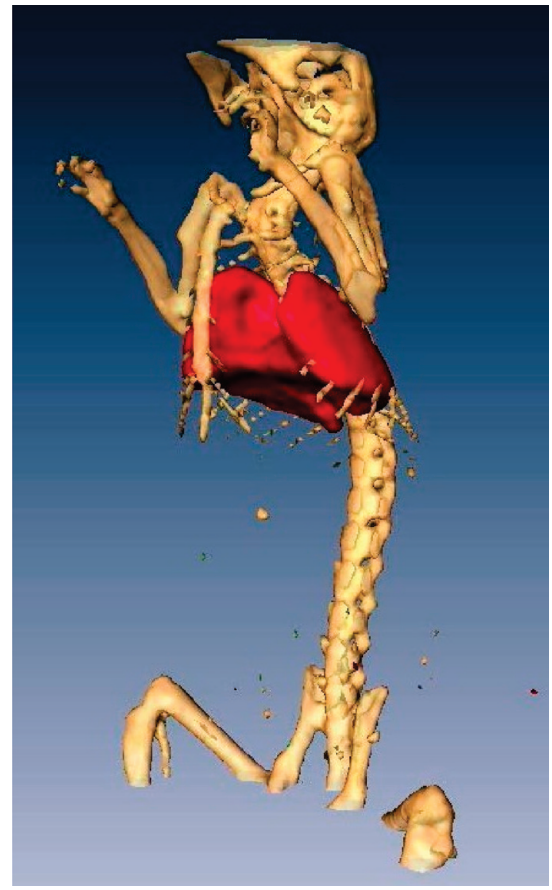

Figure 7. Surface-rendered microSPECT/CT image taken 5 min after tail vein injection of 0.2 mg of the ^{99m}Tc-radiolabeled microspheres into a healthy mouse. The radioactivity is shown in red.

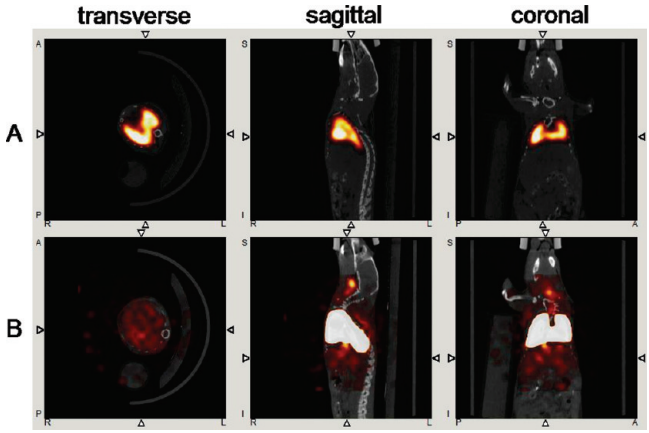

Figure 8. (A) Lung perfusion SPECT scan using ^{99m}Tc-MAA. (B) The same data but shown in the transverse direction through the liver with a much more sensitive radioactivity threshold to depict thyroid and liver activity.

Table 2. Comparison of Lung, Liver and Blood Uptake of the ^{99m}Tc-Microspheres with MAA and other Radiotracers for Lung Perfusion Imaging Described in the Literature

		lungs (%)	liver (%)	blood (%)
our results	PLA-microspheres	79.61	7.88	5.90
Miroslavov 2009[36]	^{99m}Tc(CO)$_5$I	72.00	4.50	N/A
Tsopelas 2006[40]	^{99m}Tc-SnF$_2$ colloid	88.90	5.70	N/A
Lacoeuille 2009[41]	^{99m}Tc-starch microparticles	83.40	2.40	2.08
Delgado 2000[33]	^{99m}Tc-PLGA microspheres	66.10	26.60	2.29
Lyster 1974[42]	^{99m}Tc-Sn-MAA	97.30	1.60	0.70

The control ^{99m}Tc-labeled MAA showed good trapping in the lungs at levels very close to the first reported uptake (Table 2, Lyster 1974). The small amount of activity seen in the liver and thyroid (Table 1 and Figure 8B) likely came from some of the smaller particles and from ^{99m}Tc released from the MAA in the form of pertechnetate (TcO_4^-). Pertechnetate might come from the unreacted precursor used to prepare ^{99m}Tc-MAA or from back oxidation of the postulated Tc(V) in ^{99m}Tc-MAA to Tc(VII).[2] Pertechnetate is negatively charged and similar in size to the iodine anion and, thus, gets trapped in the thyroid.

In recent years there have been several approaches to replacing ^{99m}Tc-MAA as the lung perfusion agent of choice. They are listed in terms of lung uptake as well as liver and blood distribution after 15 min in Table 2. All of the listed radiopharmaceuticals are particulates, with the exception of the only recently reported ^{99m}Tc(I) pentacarbonyl cation by Miroslavov et al.[36] Also, all particulates were radiolabeled using the reduction of ^{99m}Tc-pertechnetate with Sn(II), with the exception of our microspheres.

Although the monosized microspheres seem to be good lung perfusion agents in mice, it is not clear yet if they could be directly used in humans. According to the literature, human lung capillaries have a size of 7.5 ± 2.3 μm,[37] which is larger than the pulmonary capillaries of mice (5.7 μm).[23] It might, thus, be necessary to slightly increase the size of the microspheres for clinical use in humans to 11 or 12 μm. Particle size adjustments can be easily accomplished during the microsphere preparation with our flow focusing method by either increasing the polymer concentration or decreasing the flow ratios between the continuous and disperse phases.

Monosized microspheres made from biodegradable polymers might be useful not only for diagnostic applications, but also for therapeutic or combination applications. Similar microspheres prepared with conventional methods yielded particles of large size distributions and have been widely used in drug delivery research[38,39] and for therapeutic applications. It would, thus, only be a small step to use our monosized microspheres first to image pulmonary disease and then in a second step fill them with drugs and deliver them to the lungs for therapy. In this way, a predictable distribution can be obtained and uptake of microspheres and drugs to nontarget areas could be minimized. Because PLA and PLGA biodegradable microspheres are generally used to deliver drugs over extended times, that is, as controlled release pharmaceuticals, this would also minimize the invasiveness of this approach, as the microspheres would potentially only have to be given every few days or weeks. Applications in this form could, for example, deliver anticancer agents to the lungs to be used in combination therapy, transport antifungal drugs to treat aspergillosis, distribute antiinfectious drugs to treat pneumonia, and deliver genetically engineered materials to treat cystic fibrosis.

In addition to lung perfusion imaging, monosized radiolabeled microspheres might have additional uses in nuclear medicine. Different sizes of monodisperse microspheres can be produced with the presented flow focusing method by adjusting the flow ratio of the continuous to disperse phases (the higher the ratio, the smaller the particles) and the polymer concentration in the disperse phase (the higher the concentration, the larger the particles). Larger monosized particles sized 25−35 μm could be used in applications such as (radio-)embolization therapy, while smaller microspheres sized 1−3 μm could be used for liver and RES uptake studies. Additional applications might include bone marrow investigations (0.1 μm) and lymphoscintigraphy studies (0.03 μm). Particles at those small sizes, however, have not been produced yet with the flow focusing method; it might require significant changes in the geometry of the current device (Figure 1A) and the fluid flow conditions. Depending on the application, it would also be possible to use different radioisotopes with the presented microspheres. In addition to the use of the gamma-emitting ^{99m}Tc, the same chelating microspheres could directly bind the positron emitting ^{94m}Tc to be used in PET imaging or the beta-emitting ^{188}Re or ^{186}Re to serve as a therapeutic agent for cancer treatment. Other imaging agents such as ^{111}In or ^{68}Ga would require a change in the structure of the chelator.

Conclusion

Monosized biodegradable microspheres that can be radiolabeled through polymer-linked radiometal-specific chelators have tremendous potential to improve diagnosis and therapy in diverse areas of medicine. Adaptations of the particle size will allow for the passive targeting of many different organs and tissues, while changes in the particles' chelation chemistry will permit their imaging with different modalities. Furthermore, because the polymer materials PLA and PLGA for the preparation of these microspheres have already been extensively used for the controlled release of many different types of drugs and proteins in patients, it will be easily possible to combine both imaging and drug targeting in one platform. In a first step, one would measure the extent and location of uptake of the microspheres. Upon satisfactory biodistribution, the same microspheres containing additionally appropriate drugs would then be used in a second step to deliver therapy.

Acknowledgment. We would like to thank Chantal Saab, manager of the microSPECT/CT instrument; Rod Rhem, imaging support; and Scott McNaughton, radiopharmacist at McMaster hospital, Hamilton, Ontario, Canada, for their excellent support with the imaging studies. We also thank the Burt lab in the Faculty of Pharmaceutical Sciences at the University of British Columbia, Vancouver, Canada, for kindly providing the pegylated polymer. This research was supported by the Natural Sciences and Engineering Research Council of Canada (NSERC). The authors acknowledge the products and services provided by CMC Microsystems (www.cmc.ca) that facilitated this research, in particular, the fabrication services using the Protolyne technology from Micralyne Inc. CMC is a nonprofit corporation funded by Sciences and Engineering Research Canada (NSERC), with matching contributions from industry.

References and Notes

(1) Ercan, M. T.; Caglar, M. *Curr. Pharm. Des.* **2000**, *6*, 1085–121.
(2) Saha, G. B. *Fundamentals of Nuclear Pharmacy*, 5th ed.; Springer: New York, 2004; p. 235.
(3) Tiefenauer, L. X. In *Nanotechnology in Biology and Medicine: Methods, Devices, and Applications*; Vo-Dinh, T., Ed.; CRC Press, Taylor and Francis: Boca Raton, FL, 2007; Vol. Section D: Nanomed-.cine applications D1, pp 1−20.
(4) Mulder, W. J.; Griffioen, A. W.; Strijkers, G. J.; Cormode, D. P.; Nicolay, K.; Fayad, Z. A. *Nanomedicine* **2007**, *2*, 307–24.
(5) Vente, M. A.; Hobbelink, M. G.; van Het Schip, A. D.; Zonnenberg, B. A.; Nijsen, J. F. *Anti-Cancer Agents Med. Chem.* **2007**, *7*, 441–59.
(6) Häfeli, U. O. In *Smart Nanoparticles in Nanomedicine—The MML Series*; Arshady, R., Kono, K., Eds.; Kentus Books: London, U.K., 2006; Vol. 8, pp 77−126.
(7) Arshady, R.; Monshipouri, M. In *Microspheres, Microcapsules & Liposomes: Medical and Biotechnology Applications*; Arshady, R., Ed.; Kentus: London, 2001; Vol. MML 2, pp 410−414.
(8) Wattendorf, U.; Merkle, H. P. *J. Pharm. Sci.* **2008**, *97*, 4655–69.
(9) von Behrens, W. E.; Oates, G. C. U.S. Patent 3,871,770, 1975.
(10) Ganan-Calvo, A. M.; Martin-Banderas, L.; Gonzalez-Prieto, R.; Rodriguez-Gil, A.; Berdun-Alvarez, T.; Cebolla, A.; Chavez, S.; Flores-Mosquera, M. *Int. J. Pharm.* **2006**, *324*, 19–26.
(11) Berkland, C.; Pollauf, E.; Varde, N.; Pack, D. W.; Kim, K. K. *Pharm. Res.* **2007**, *24*, 1007–1013.
(12) Holgado, M. A.; Arias, J. L.; Cozar, M. J.; Alvarez-Fuentes, J.; Ganan-Calvo, A. M.; Fernandez-Arevalo, M. *Int. J. Pharm.* **2008**, *358*, 27–35.
(13) Rhodes, B. A.; Zolle, I.; Buchanan, J. W.; Wagner, H. N. *Radiology* **1969**, *92*, 1453–1460.
(14) Martin-Banderas, L.; Flores-Mosquera, M.; Riesco-Chueca, P.; Rodriguez-Gil, A.; Cebolla, A.; Chavez, S.; Ganan-Calvo, A. M. *Small* **2005**, *1*, 688–92.
(15) Schneider, T.; Zhao, H.; Jackson, J. K.; Chapman, G. H.; Dykes, J.; Häfeli, U. O. *J. Pharm. Sci.* **2008**, *97*, 4943–4954.
(16) Cleland, J. L. *Biotechnol. Prog.* **1998**, *14*, 102–107.
(17) Freitas, S.; Merkle, H. P.; Gander, B. *J. Controlled Release* **2005**, *102*, 313–32.
(18) Saatchi, K.; Häfeli, U. O. *Dalton Trans.* **2007**, *39*, 4439–4445.
(19) Zastre, J.; Jackson, J.; Bajwa, M.; Liggins, R.; Iqbal, F.; Burt, H. *Eur. J. Pharm. Biopharm.* **2002**, *54*, 299–309.
(20) Pieters, R.; Huismans, D. R.; Leyva, A.; Veerman, A. J. P. *Br. J. Cancer* **1989**, *59*, 217–220.
(21) Giard, D. J.; Aaronson, S. A.; Todaro, G. J.; Arnstein, P.; Kersey, J. H.; Dosik, H.; Parks, W. P. *J. Natl. Cancer Inst.* **1973**, *51*, 1417–23.
(22) Saatchi, K.; Häfeli, U. O. *Bioconjug. Chem.* **2009**, *20*, 1209–1217.
(23) Geelhaar, A.; Weibel, E. R. *Respir. Physiol.* **1971**, *11*, 354–66.
(24) Vochelle, D. *Semin. Cutaneous Med. Surg.* **2004**, *23*, 223–6.
(25) Athanasiou, K. A.; Niederauer, G. G.; Agrawal, C. M. *Biomaterials* **1996**, *17*, 93–102.
(26) Yamaguchi, K.; Anderson, J. M. *J. Controlled Release* **1993**, *24*, 81–93.
(27) Fournier, E.; Passirani, C.; Montero-Menei, C. N.; Benoit, J. P. *Biomaterials* **2003**, *24*, 3311–31.
(28) Emerich, D. F.; Tracy, M. A.; Ward, K. L.; Figueiredo, M.; Qian, R.; Henschel, C.; Bartus, R. T. *Cell Transplant.* **1999**, *8*, 47–58.
(29) DeLand, F. H. *J. Nucl. Med.* **1966**, *7*, 883–95.
(30) Häfeli, U. O.; Roberts, W. K.; Pauer, G. J.; Kraeft, S. K.; Macklis, R. M. *Appl. Radiat. Isot.* **2001**, *54*, 869–879.
(31) Horsfield, K. *Circ. Res.* **1978**, *42*, 593–7.
(32) Davis, M. A. In *Radiopharmaceuticals*; Subramaniam, B., Rhodes, B., Cooper, D. R., Sodd, V. J., Eds.; Society of Nuclear Medicine: Reston, VA, 1975; pp 267−281.
(33) Delgado, A.; Soriano, I.; Sanchez, E.; Oliva, M.; Evora, C. *Eur. J. Pharm. Biopharm.* **2000**, *50*, 227–236.
(34) Mallol, J.; Diaz, R. V. *Nucl. Med. Commun.* **1997**, *18*, 87–8.
(35) Alberto, R.; Schibli, R.; Egli, A.; Schubiger, P. A.; Abram, U.; Kaden, T. A. *J. Am. Chem. Soc.* **1998**, *120*, 7987–7988.
(36) Miroslavov, A. E.; Gorshkov, N. I.; Lumpov, A. L.; Yalfimov, A. N.; Suglobov, D. N.; Ellis, B. L.; Braddock, R.; Smith, A. M.; Prescott, M. C.; Lawson, R. S.; Sharma, H. L. *Nucl. Med. Biol.* **2009**, *36*, 73–79.
(37) Doerschuk, C. M.; Beyers, N.; Coxson, H. O.; Wiggs, B.; Hogg, J. C. *J. Appl. Physiol.* **1993**, *74*, 3040–3045.
(38) Wischke, C.; Schwendeman, S. P. *Int. J. Pharm.* **2008**, *364*, 298–327.
(39) Mohamed, F.; van der Walle, C. F. *J. Pharm. Sci.* **2008**, *97*, 71–87.
(40) Tsopelas, C.; Batholomeusz, F. D. L. *J. Labelled Compd. Radiopharm.* **2006**, *49*, 367–375.
(41) Lacoeuille, F.; Hindre, F.; Denizot, B.; Bouchet, F.; Legras, P.; Couturier, O.; Askienazy, S.; Benoit, J. P.; Le Jeune, J. J. *Eur. J. Nucl. Med. Mol. Imaging* **2010**, *37*, 146–155.
(42) Lyster, D. M.; Scott, J. R.; Mincey, E. K.; Morrison, R. T. *J. Nucl. Med.* **1974**, *15*, 198–199.

BM9010722